

Contribution to the  
Fourth OECD Workshop on Iodine Chemistry in Reactor Safety  
PSI, Villigen, Switzerland, 10 - 12 June 1996

## FURTHER ASSESSMENT OF THE CHEMICAL MODELLING OF IODINE IN IMPAIR 3 CODE USING ACE/RTF DATA

R.C. Cripps and S. Guntay<sup>1</sup>

This paper introduces the assessment of the computer code IMPAIR 3 (Iodine Matter Partitioning And Iodine Release) which simulates physical and chemical iodine processes in a LWR containment with one or more compartments under conditions relevant to a severe accident in a nuclear reactor. The first version was published in 1992 to replace both the multi-compartment code IMPAIR 2/M and the single-compartment code IMPAIR 2.2.

IMPAIR 2.2 was restricted to a single pH value specified before program execution and precluded any variation of pH or calculation of H<sup>+</sup> changes during program execution. This restriction is removed in IMPAIR 3. Results of the IMPAIR 2.2 assessment using ACE/RTF Test 2 and the acidic phase of Test 3 B data were presented at the 3rd CSNI Workshop.

The purpose of the current assessment is to verify the IMPAIR 3 capability to follow the whole test duration with changing boundary conditions. Besides revisiting ACE/RTF Test 3B, Test 4 data were also used for the current assessment. A limited data analysis was conducted using the outcome of the current ACEX iodine work to understand the iodine behaviour observed during these tests. This paper presents comparisons of the predicted results with the test data. The code capabilities are demonstrated to focus on still unresolved modelling problems. The unclear behaviour observed in the gaseous molecular iodine behaviour and its inconclusive effect on the calculated behaviour in the acidic phase of the Test 4 and importance of the catalytic effect of stainless steel are also indicated.

<sup>1</sup> Paul Scherrer Institut, Laboratory for Safety and Accident Research, 5232 Villigen PSI, Switzerland

## 1. INTRODUCTION

The IMPAIR 3 (Iodine Matter, Partitioning And Iodine Release) Computer Code simulates physical and chemical processes in one or more compartments of a LWR containment during a hypothetical severe accident. This version is an update [1] of the first multi-compartment code IMPAIR 2/M presented at the last Workshop [2]. It contains the basic physical and chemical models as the earlier single-compartment code IMPAIR 2.2 [3] with the added ability to calculate iodine species behaviour in dry compartments, to represent transport of species between compartments and to calculate the release of airborne iodine species into the environment. It is already integrated into containment codes such as CONTAIN and FIPLOC /M, so that thermal-hydraulic and aerosol behaviour can be directly considered.

The purpose of the current assessment is to verify the IMPAIR 3 capability to follow the whole test duration with changing boundary conditions and to expand the past IMPAIR 2.2 assessment work [5] using the ACE/RTF data obtained from Test 2 and the acidic phase of Test 3B. Besides revisiting the ACE/RTF Tests 3B, Test 4 was also simulated. A limited data analysis conducted indicated several difficulties in understanding the behaviour observed. Lack of error bands on the measured quantities is the main reason for the difficulties. This paper presents comparisons of the predicted results with the test data. The code capabilities are demonstrated to focus on still unresolved modelling problems. The unclear behaviour observed in the gaseous molecular iodine behaviour in the acidic phase of the Test 4 and importance of the catalytic effect of stainless steel are also indicated.

## 2. METHODOLOGY

Modelling approach adopted in the IMPAIR 3 Code is a phenomenological treatment of iodine chemistry. Phenomenological modelling is based on correlations with data obtained from integral experiments. Relatively crude models involving few empirical equations are often used to represent the composite effect of a large number of competing and sequential reactions (e.g. iodine radiolysis reactions).

The main advantage in adopting this method over the detailed mechanistic modelling is its fast running feature. It is especially important for CPU-intensive multiple compartment applications. The main disadvantage of this method is that the validity of the models is limited to the experimental data base for which the models are assessed. The IMPAIR 3 Code and its predecessor have been assessed using the ACE/RTF data base.

A detailed description of the models used in IMPAIR 3 Code can be found in the handbook [1].

## 3. MODELLING FEATURES

Both radiolysis and deposition played a significant role in ACE/RTF Tests 3B and 4 during the acidic period (pH 5). IMPAIR 3 uses, as before, a simple empirical equation to model the overall effect of a large number of radiolysis reactions for the oxidation of iodide to molecular iodine [1]. The rate and exponent in this equation for the forward and reverse reactions were adjusted until the calculated and measured iodide concentrations showed a close agreement for the complete pH range of the Test 3B. The values were then kept to be the same for the Test 4 simulation.

### 3.1 Deposition of $I_2$ on paint surfaces in the gas space

The equations modelling the dry surface deposition are unchanged since IMPAIR 2.2 assessment [5]. The RTF test vessel was coated with Keeler & Long self-priming epoxy-amine enamel #4500 for ACE/RTF Test 1 to Test 3. A deposition rate constant of  $0.19 \text{ cm s}^{-1}$  was estimated at operating temperature of Test 3B ( $60^\circ\text{C}$ ) using the experimental data [6] obtained at  $80^\circ\text{C}$  for this paint type. This compares favourably with the value ( $0.25 \text{ cm s}^{-1}$ ) which was obtained during the previous assessment by adjusting the rate constant until the IMPAIR 2.2 Code results modestly correlated the Test 3B data.

Since the paint type might be different in any IMPAIR 3 application, appropriate rate constants for the deposition on the given painted surfaces at relevant thermal-hydraulic conditions (temperature and humidity) should be provided to the code as input data.

### 3.2 Deposition of $I_2$ on immersed stainless steel

Data from a recent experimental work [7] indicated that a zero steady-state  $I_2$  loading on the immersed steel surface occurred due to a rapid temperature-dependent reduction to iodide.

Contrary to the data in [7], a minimum surface deposition (about  $4.0 \times 10^{-7} \text{ mole.m}^{-2}$ ) was reported in Test 4 results and was about 100 times less than the estimate for the gas space surface loading. Hence the current code model simulates deposition and reduction to dissolved iodide.

### 3.3 Deposition of $I_2$ on gas space stainless steel

A deposition rate constant of  $0.1 \text{ cm s}^{-1}$  at  $60^\circ\text{C}$  was estimated using the data set provided in the literature [8]. A revolatilisation rate of  $9.0 \times 10^{-6} \text{ s}^{-1}$  was found by slightly adjusting the rate constant used during the previous assessment to match the measured gas space  $I_2$  concentrations. The current model does not consider surface saturation or humidity effects on deposition.

### 3.4 Partitioning of hypoiodous acid

An interface model for mass transfer of HOI species between the gas and water spaces was added to the code. The model is consisted of a differential equation analogous to that of  $I_2$ . An empirical formula, derived from an earlier work [9], is built to calculate the HOI partition coefficient. A partitioning coefficient of about 380 is predicted at the sump water temperature of  $60^\circ\text{C}$ .

### 3.5 Formation and dissociation of the $I_3^-$ species

The formation and dissociation of the  $I_3^-$  species reaction are significant at higher iodide concentrations ( $>1.0 \times 10^{-4} \text{ mole.dm}^{-3}$ ) due to evaporation of sumps. Although not important for the iodide concentrations used in these tests, a model was added to the code for completeness.

### 3.6 Organoiodine modelling

IMPAIR 3 modelling of methyl iodide formation (homogeneous and on paint surfaces), depletion (hydrolysis and radiolysis) and interface mass transfer is identical to the one built in IMPAIR 2.2 Code. An analogous set of models was built in IMPAIR 3 to attempt to simulate behaviour of all organoiodides with more than one carbon atom (Higher Molecular Weight organoiodides). HMWI and methyl iodide reaction mechanisms are assumed to be identical. It is likely that a large number of organoiodide species is simultaneously present in a given scenario. However, the separate effects data base, apart from hydrolysis rate constants ( $\text{H}_2\text{O}$  and  $\text{OH}^-$ ) [10,11], are very limited. Reaction of iodine with organic material is dependent on the rate constants as well as initially available organic residuals in the sump water. The initial amount of residual organic material in the RTF experiments is not known. The rate constants have not been assessed with other data sets. Therefore, the current assessment using the RTF 3 B and 4 Test data is an attempt to demonstrate the status of the organoiodide modelling.

## 4. CODE ASSESSMENT

The data base produced from the Phase B of the International Advanced Containment Experiments (ACE) Project [4] has been used for the basis of the current and the past IMPAIR assessment. The experiments were performed at the Radioiodine Test Facility (RTF) at AECL Research, Whiteshell Laboratories, Canada. A summary of the experimental conditions is shown in Table 1.

**Table 1. ACE/RTF Tests 1 to 4, experimental conditions**

Experiment						Dose Rate kGy/h	Test conditions				Surface type
							Initial concentration: $1.0 \times 10^{-5} \text{ mol.l}^{-1}$				
RTF	A	B	C	D	E		*	*	*	**	
1	CsI	$\text{CH}_3\text{I}$	I <sub>2</sub>			none	9/173			80	Epoxy painted carbon steel
2	CsI	$\text{CH}_3\text{I}$	I <sub>2</sub>			2.0	9/122 ***			60	Epoxy painted carbon steel
3	$\text{CH}_3\text{I}$	CsI	I <sub>2</sub>	$\text{CH}_3\text{I}$	I <sub>2</sub>	2.0	5.5/73 ****	9/51		60	Epoxy painted carbon steel
4	CsI					2.0	9/145	5.5/110	9/53	60	Stainless steel

\*: pH and time (h)

\*\* : temperature (°C)    \*\*\* : Test A, CsI solution    \*\*\*\*: Test B: CsI solution

Uncertainties in the measurements and error bands were not provided for the measured quantities in the ACE/RTF documents. Lack of this data made the interpretation of the measured behaviour very difficult to reach conclusive decisions about the trends.

#### **4.1 Previous Assessment Work**

The last single compartment code, IMPAIR 2.2, was previously validated using the ACE/RTF 2A and the acidic phase of Test 3B data. The aim was to achieve a first validation of the phenomenological models, especially the pH-sensitive models such as the radiolytic oxidation of iodide ions in solution. A good agreement for most species, except the  $I_2$  in the water space, with each set of test data at constant pH (pH 9.0 and 5.5, respectively) was obtained. The IMPAIR 2.2 Code had overestimated the  $I_2$  water space concentration. The results were presented at the Third CSNI Workshop on Iodine Chemistry in Reactor Safety, September 11-13, 1991 in Tokai-mura, Japan [5].

#### **4.2 Assessment of IMPAIR 3 Code with ACE/RTF Test 3 and 4 databases**

The aims of the current assessment are:

1. To show the calculated effects of an abrupt programmed change of pH and demonstrate the capability of the code to follow the changing pH during the test period as well as to investigate possible long term effects of the changing pH on the iodine behaviour. Due to the inability of the IMPAIR 2.2 Code to follow the time dependent boundary conditions, possible long term or history effects on the iodine behaviour could not be simulated in the previous assessment, after the pH was ramped to 9.
2. To adjust pH-sensitivity of the empirical equation in the code which governs the global radiation-induced oxidation of iodide to achieve a close agreement with the measured iodide concentrations for each of the entire ACE/RTF Tests 3B and 4.
3. To compare the surface loadings calculated on paint and stainless steel surfaces in the gas space with the ACE/RTF TEST 3 and 4 deposition data.

Initial calculations, employing the rate constants used in the previous assessment made for ACE/RTF Test 3B, have shown a divergence between the experimental and calculated  $I_2$  water space concentrations when the pH was ramped to 9. This indicated that the empirical rate constants used in the previous assessment were clearly not optimal for the entire test where the pH was changed. Hence in the current assessment ACE/RTF Test 3B calculations were repeated.

#### **4.3 Code Assessment using ACE/RTF Test 3 data**

##### **4.3.1 Iodide concentrations**

As in the previous IMPAIR 2.2 Code assessment, radiolysis rate constants were adjusted to obtain a close agreement between the measured and calculated iodide concentrations. However, the adjustment was made but this time for the entire test. In the current assessment, the pH-sensitivity was increased to reach a close fit for both Test 3B and Test 4 data sets. On ramping to pH 9, a slight divergence was obtained (Figure 1), leading to an underestimation

of  $I_2$ , in the water space (Figure 2). A significant portion of  $I_2$ , which was transported from the water space into the gas space, was deposited on the wall surfaces as shown in Figure 6.

#### 4.3.2 Molecular iodine concentrations in the water and gas spaces

Good agreements for the water (Figure 2) and gas space molecular iodide concentrations (Figure 3) were obtained and hence the calculated partition coefficient for  $I_2$  (Figure 4) agrees very well with the deduced one based on the measured data.

#### 4.3.3 Total partition coefficient

The calculated and measured total partition coefficients are shown in Figure 5 to indicate the effect of other volatile iodine species ( $CH_3I$ , HMWI and HOI) besides  $I_2$ . The underestimation of volatile iodine species during the acidic period was not significant.

#### 4.3.4 Deposition on the paint surfaces in the gas space

A close agreement was achieved for the maximum surface loading, as shown in Figure 6, although some underprediction occurred during the first 10000 s of the simulation. However, it is difficult to conclude the extend of the underprediction due to the lack of the error band on the experimental data.

#### 4.3.5 Iodate concentrations

Figure 7 presents a comparison of calculated and measured iodate concentrations. The measured and calculated concentration trends were quite different despite absolute values of the concentrations are of similar order of magnitude. The experimental curve showed no particular trend, apart from a slight decreasing concentration. The variation in the experimental values are inconclusive. It is conceivable that possible uncertainties in the measured values could have masked the true behaviour of the reaction. It is, therefore, difficult to interpret whether the lower iodate concentration after the pH change showed a trend, because the difference between iodate concentrations measured before and after the pH change could be within the measurement uncertainties. If this is the case, the iodate concentration throughout the test remained approximately constant. The calculated trend showed a prominent fast rise (burst) as contrary to the measured data when the pH was increased to 9. The code predicted a rapid hydrolysis and disproportionation of  $I_2$  that was generated during the acidic period. Although the relative importance of the calculated hydrolysis and the Dushman reaction (iodate depletion reaction) were reversed at pH 9, the computed relatively high iodate "peak concentration" could be attributed to the overemphasised hydrolysis effect in the code or an unknown mechanism was depleting the iodate in the test.

#### 4.3.6 Organoiodide results

Figure 8 and 9 present a comparison of the calculated and measured total organoiodide concentrations in the gas and water spaces respectively. The good agreements presented in these figures conclude that the organic iodine modelling, although, the rate constants were

not assessed previously, and the initial organic residuals were only estimates, looks promising.

#### 4.4 Code Assessment using ACE/RTF Test 4 data

##### 4.4.1 Iodide Concentrations

Figure 10 presents the measured and calculated iodide concentrations. Both concentrations stayed practically constant until about  $5 \times 10^5$  s at pH 9. This stable behaviour was due to the negligible radiolytic oxidation of iodide at high pH. Consequently a very close agreement was expected and achieved.

After ramping to pH 5.2 (acidic period:  $\sim 500,000$  s to  $\sim 940,000$  s), a continued close agreement was only obtained after adjustment of the rate and exponent constants in the radiolytic iodide oxidation equation.

The IMPAIR Code simulates a radiation-independent reverse reaction, which reduces  $I_2$  in solution to iodide. As described above, the code contains a model to reduce  $I_2$  deposited on immersed steel surfaces to metal iodides. These reaction products are considered to be immediately dissolved in the water phase. A 10 fold larger rate constant for the higher reverse reaction was used, compared with the values used for Test 3B (paint surface), to achieve a good agreement. It is feasible that the metal ions may have influenced the reverse reaction. This shows a clear need to explicitly model radiation chemical reactions of metal ions released from steel surfaces.

Upon ramping the pH back to 9, a slight overestimation of the iodide concentration was calculated. This may be due to the overpredicted  $I_2$  concentration from the previous acidic period, which is subjected to hydrolysis and disproportionation.

##### 4.4.2 Water and gas space molecular iodine concentrations

The molecular iodine concentrations in the water (Figure 11) and in the gas spaces (Figure 12) were respectively overestimated and underestimated by about an order of magnitude during the acidic period. A close agreement for the gas space concentrations could only be obtained by selecting a deposition rate for the gas space steel surfaces of about two orders of magnitude less than the literature value. Using this low deposition rate, the molecular iodine in the water space was then overestimated by more than two orders of magnitude.

##### 4.4.3 Calculated and measured partition coefficients for molecular iodine

Figure 13 shows a comparison between the measured and calculated molecular iodine partition coefficients. The calculated values are based on the computed bulk  $I_2$  concentrations in the water and gas spaces. The code calculates the equilibrium partition coefficient for  $I_2$  using an empirical formula derived from a previous work [9]. This value is about 20 at 60°C. The calculated equilibrium value of the partition coefficient was maintained throughout the first alkaline period and with some slight increase until the end of the acidic period.

After ramping the pH back to 9, the calculated partition coefficient reduced rapidly to about 0.6. This was probably due to rapid hydrolysis depleting the water space  $I_2$  concentrations, followed by a slower recovery by  $I_2$  transfer, through the gas space, from the gaseous  $I_2$  loaded on the steel surfaces in the gas space. A complete recovery, presumably to the equilibrium value, would only be reached by continuing the code execution.

The measured  $I_2$  partition coefficient stayed also at a constant value of about 10 during the first pH 9 period. However, in contrast to the code prediction, it fell rapidly to less than 0.1 in the acidic period and remained at about 1 for the remainder of the test. This was reflected directly in the overprediction of the water space molecular iodine concentration (Figure 11) and underprediction of the gas space concentration (Figure 12).

Since the measured  $I_2$  concentration in the gas space is higher than in the water space during the acidic period, it is not clear at all whether a technical artefact in the measurement technique or alternatively a physical process caused this excessively low water space concentration. No reason is provided in the data report for this phenomenon.

#### **4.4.4 Calculated and measured total partition coefficients**

The total partition coefficients are compared in Figure 14. The difference between the calculated and measured total partition coefficient during the first alkaline period is less than an order of magnitude. The acidic period indicated a decreasing underestimation of volatile species. After pH ramping to 9, a good agreement was obtained. Comparison of the absolute values of the total and  $I_2$  only partitioning coefficients indicated that a large fraction of the iodine inventory was predicted to remain in the water and on gas space surfaces as in the experiment.

#### **4.4.5 Deposition on gas space steel surfaces**

Since the vessel walls were washed down at the end of the Test 4, which released 28% of the initially available iodine inventory, the maximum Test 4 surface concentration was estimated to be  $4 \times 10^{-5}$  mole.m<sup>-2</sup>. Figure 15 shows that the maximum calculated surface loading is very close to the maximum load estimate during the acidic period.

#### **4.4.6 Iodate concentration in the water space.**

A close agreement was achieved as seen in Figure 16 during the first alkaline period before the Dushmann reaction became significant during the acidic period. A “burst” of iodate was predicted after returning to pH 9, as found in the RTF 3B simulation. The rapid rise was caused by hydrolysis and disproportionation of the overpredicted  $I_2$ , which was generated during the previous acidic period. Unavailability of the experimental error bands made it difficult to determine the extend of the overestimation.

#### **4.4.7 Organoiodine results**

In Test 4, impurities formed the only source of organoiodine, since a stainless steel surface replaces the epoxy-paint surfaces of the previous tests. Considering the invalidated rate constants for the organoiodine formation and uncertainties in the amount of organic impurities assumed in the input data, the good agreements shown in Figures 17 and 18 indicate that provided a minimum initial amount of impurities necessary to sustain the organic iodine interaction, the rate constants used in the assessment did indeed a good job.



## 5. CONCLUSIONS

The calculated results for both RTF Test 3B and Test 4 confirm that IMPAIR 3 continues to reproduce the results produced by its predecessor. It is demonstrated that the code can follow the changing boundary conditions and can reproduce most of the trends seen in the experimental data.

Unfortunately the lack of experimental uncertainties on measured concentrations did not make it possible to satisfactorily assess all the code models relevant for RTF test data.

In particular, the iodide burst calculated for both tests when the pH was changed from 5 to 9 was largely overpredicted. The measured Test 4 molecular iodine concentrations in the water space have shown a large decrease when the pH was changed from 9 to 5, which resulted in a partition coefficient for  $I_2$  of 0.1. This may be associated either with the measurement technique or with a physical process that is currently not understood. Similarly, the code indicated that the equilibrium value of the partition coefficient could be obtained in the long run after the pH was changed from 5 to 9 due to the release of the deposited molecular iodine on the steel surface although no such trend was observed in the experiment. Therefore, it could be argued that the RTF data should be compared with the independent data, if available, to understand the trends and phenomena observed.

Generally the code models the iodine behaviour observed during the ACE/RTF tests correctly. However, more accurate data are needed to validate and expand the validity range of the current IMPAIR 3 models. The need to extend the modelling to include the effect of metal ions on the radiolytic oxidation of iodide reaction is emerging from the analysis.

## 6. REFERENCES

[1] Guntay S.; Cripps R., IMPAIR /3: A Computer program to Analyse the Iodine Behaviour in Multi-Compartments of a LWR Containment , PSI-Bericht No. 128 (1992), Paul Scherrer Institute, Villigen, Switzerland.

[2] Guntay S., IMPAIR-2/M/: An extension of the computer program IMPAIR-2 to analyse the iodine behaviour in multi-compartments of a LWR containment, Internal publication, Paul Scherrer Institute, Villigen, Switzerland.

[3] Cripps R.; Furrer M.; Hellmann S. and Funke F., User's handbook for the iodine severe accident Code IMPAIR 2.2, PSI-Bericht No. 114 (1992) , Paul Scherrer Institute, Switzerland.

[4] Kupferschmidt W.C.H.; Ball J.M; Buttazoni J.B; Evans G.J; Jobe D.J; Melnyk A.J.; Palson A.S.; Portman R and Sanipelli G.G. , Final Report on the ACE/RTF Experiments, ACE-TR-B3 (1992) July , Research Chemistry Branch, AECL, Whiteshell Nuclear Research Establishment, Pinawa, Manitoba, Canada.

[5] Furrer M. and Cripps R.C., Validation of IMPAIR 2 Code using ACE-Test results from the Radioiodine Test Facility (RTF), Proc. Third CSNI Workshop on Iodine Chemistry in Reactor Safety, Tokai-mura, Japan (1991).

[6] Evans G.J. and Palson A.S., The Absorption of I<sub>2</sub> vapour by Epoxy Paint at 80°C, ACE-TR-B11, 1991, Research Chemistry Branch, AECL, Whiteshell Nuclear Research Establishment, Pinawa, Manitoba, Canada.

[7] Funke F; Greger G.-U; Hellmann S; Bleier A and Morell W., Iodine/Steel Reactions under Severe Accident Conditions in LWR's, Proc. Third International Conference on Containment and Design, Toronto, Ontario, Canada (1994).

[8] Evans G.J. Deir C. and Ball J.M., The Retention of Iodine on Stainless Steel Sample Lines, Proc. 23rd DOE/NRC Nuclear Air Cleaning Conference, NUREG/CP-0141, Conf-940738, p279 (1995).

[9] Furrer M., Cripps R.C. and Gubler R., Measurement of the Iodine Partition Coefficient, Nucl. Technol. 70, 290-293, (1985).

[10] Buxton G.V., Greenstock C.L., Helman W.P. and Ross A.B., Critical Review of Rate Constants for Reactions of Hydrated Electrons, Hydrogen Atoms and Hydroxyl Radicals (OH/O<sup>-</sup>) in Aqueous Solution, J. Phys. Chem. Ref. Data, Vol. 17, No. 2,1.

[11] Borkowski R., Untersuchungen zum chemischen Verhalten des Methyljodides bei schweren Störfällen in Druckwasserreaktoren, KfK Report 3968.

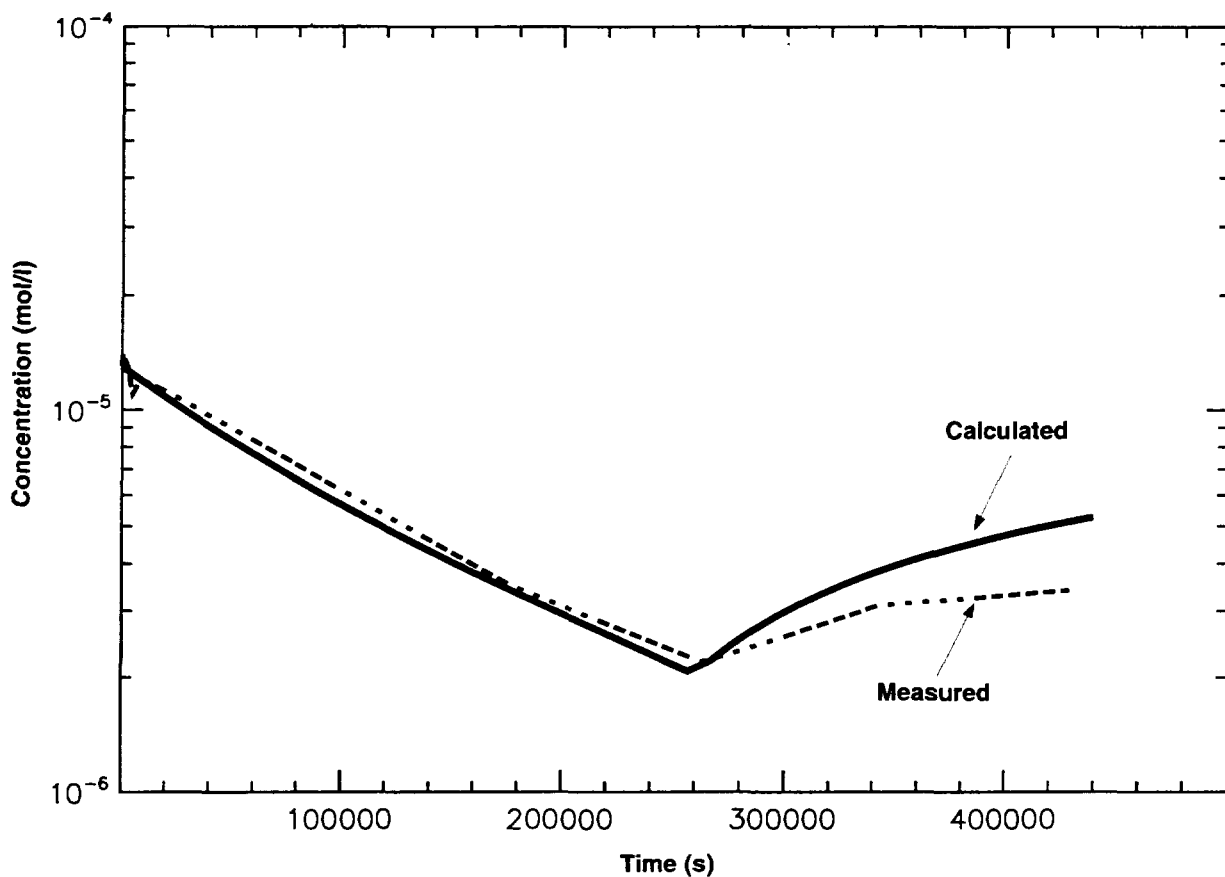


Figure 1: ACE/RTF 3B: Iodide Concentrations in the Water Space

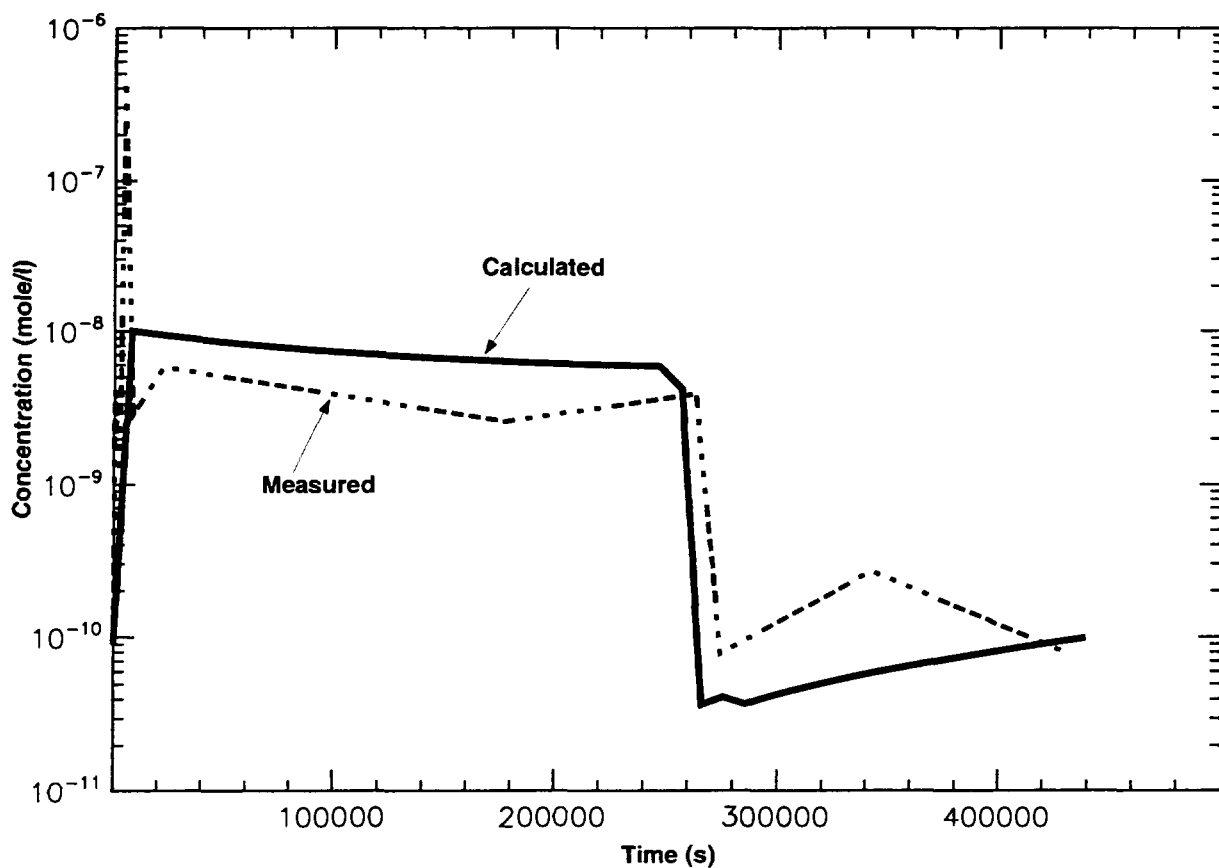


Figure 2: ACE/RTF 3B: Molecular Iodine Concentrations in Water Space

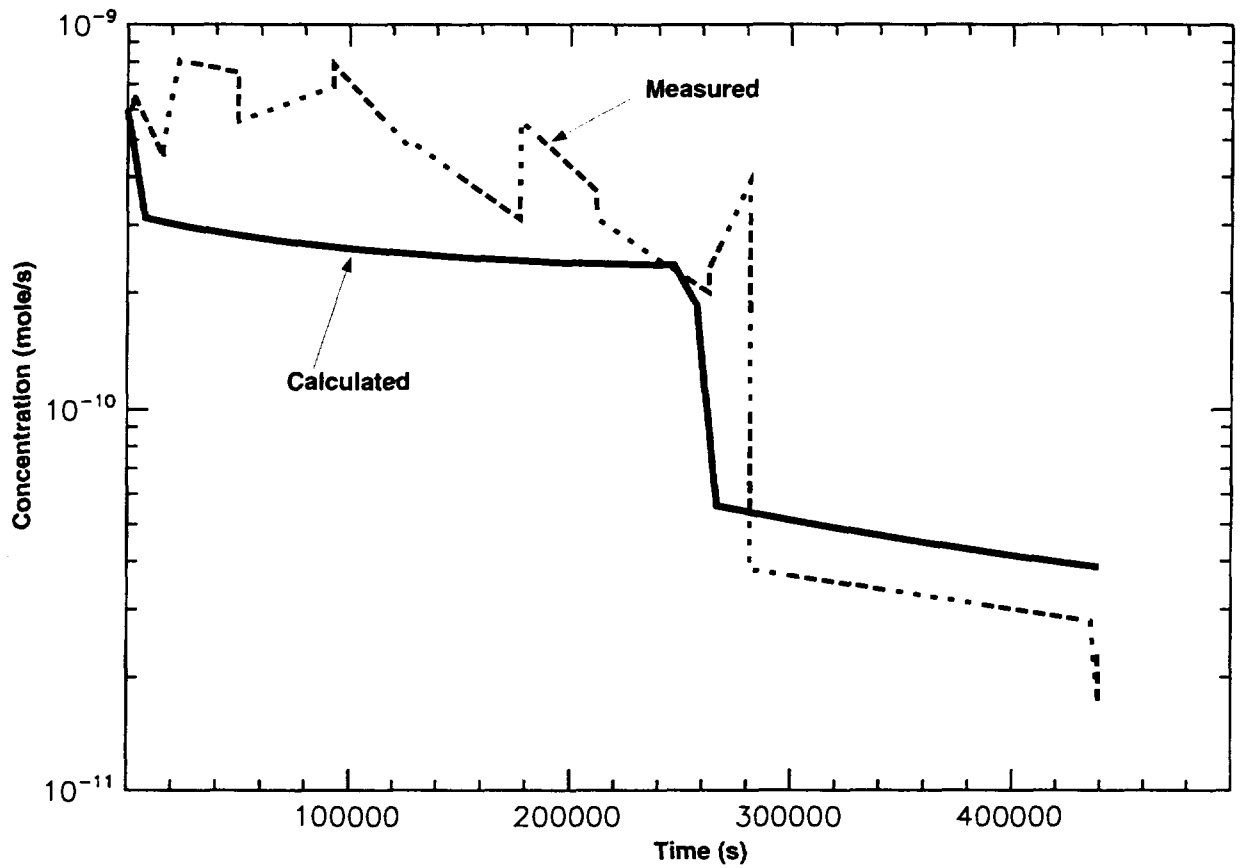


Figure 3: ACE/RTF 3B: Molecular Iodine Concentrations in the Gas Space

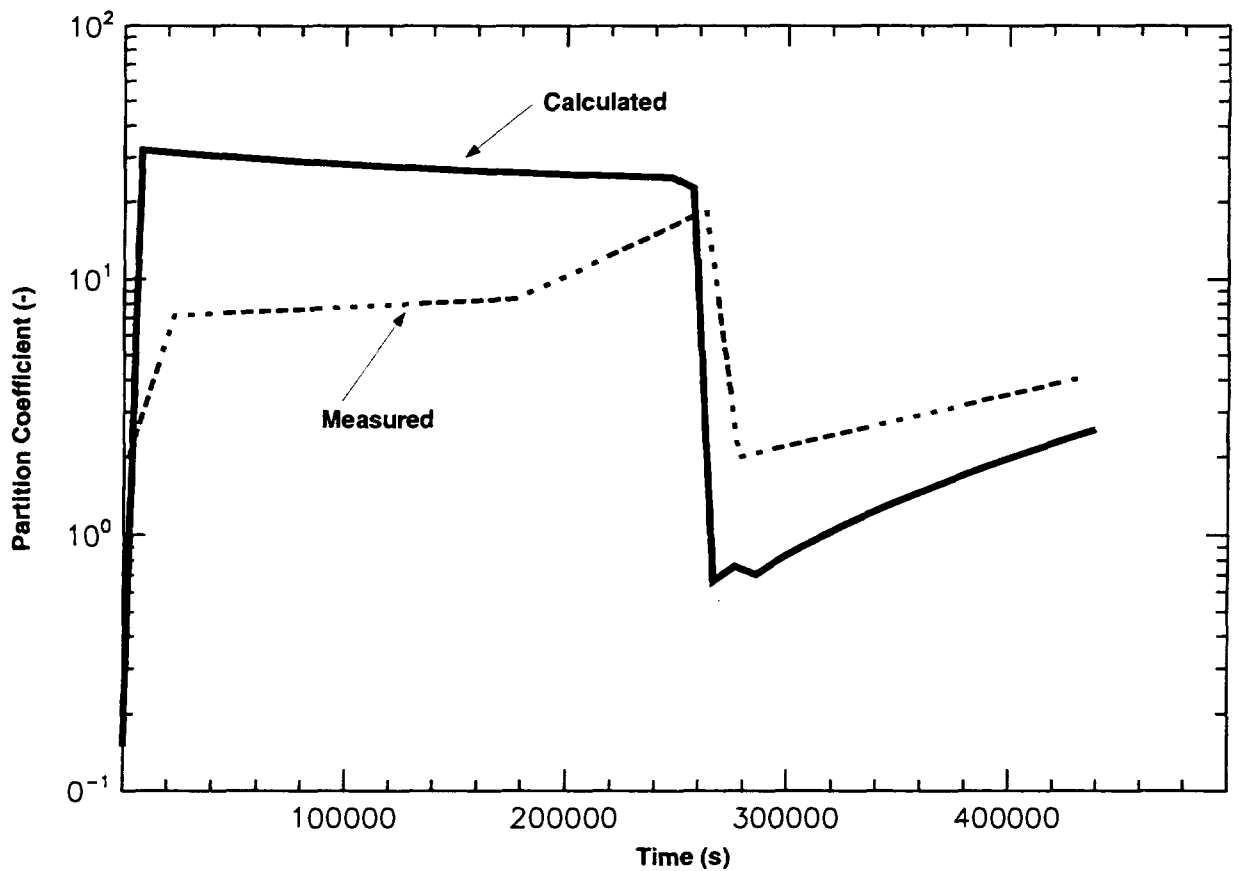


Figure 4: ACE/RTF 3B: Molecular Iodine Partition Coefficients

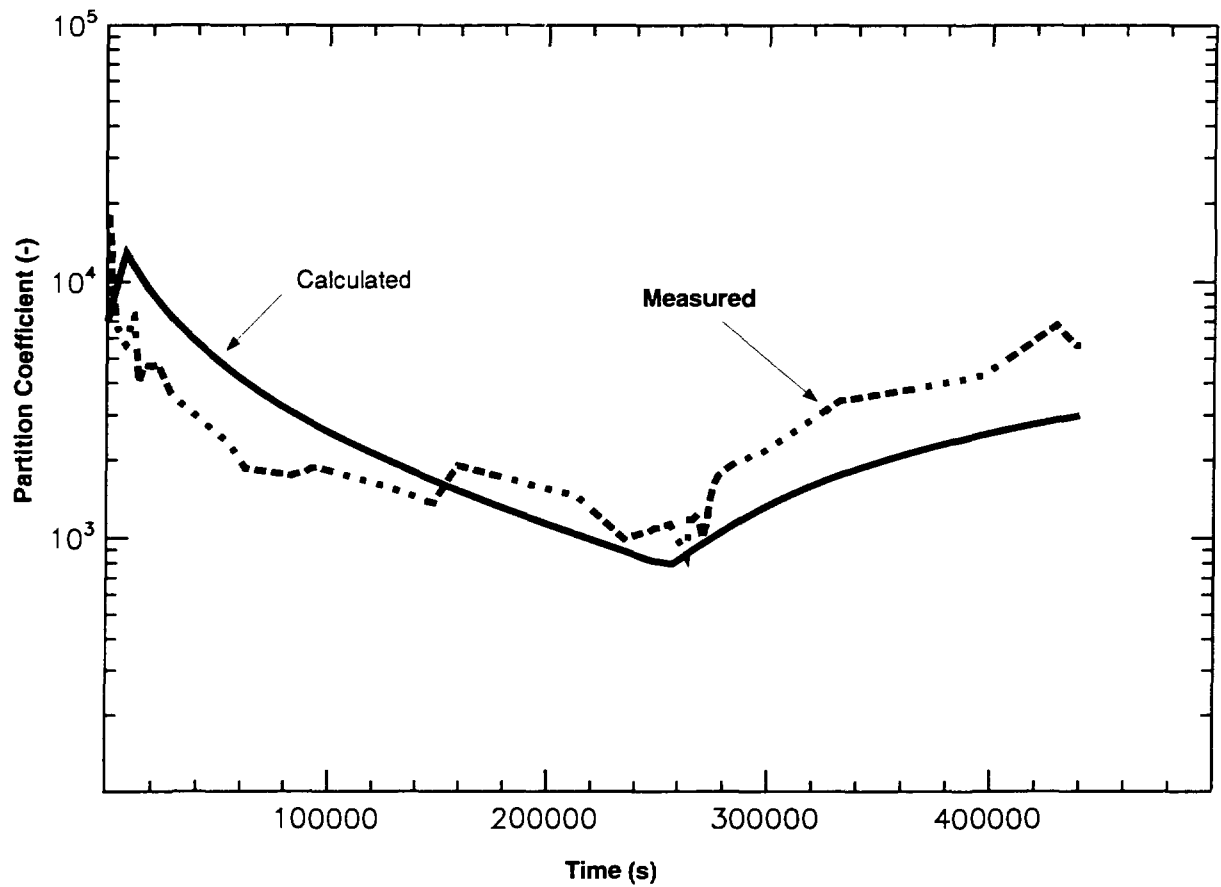


Figure 5: ACE/RTF 3B: Total iodine Partition Coefficients

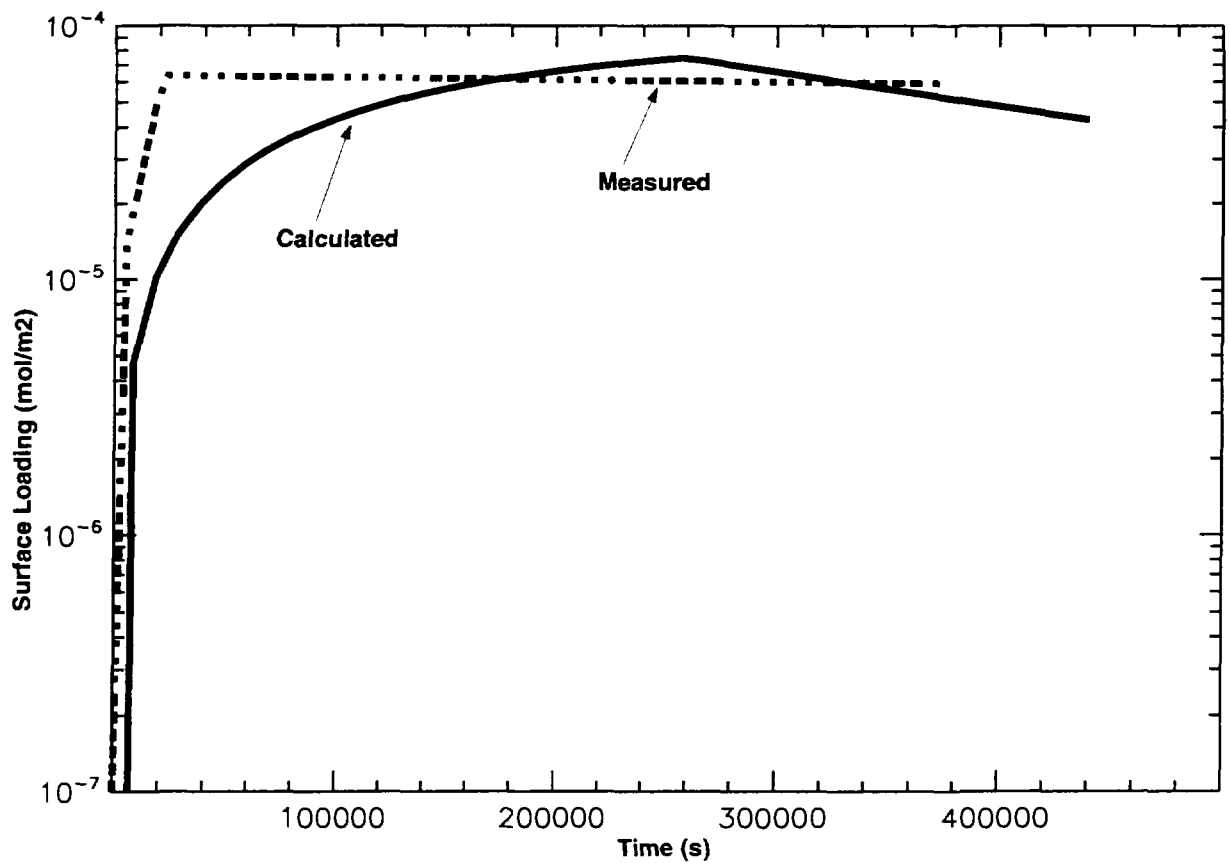


Figure 6: ACE/RTF3: Surface Loadings on the Paint Surface in the Gas Space

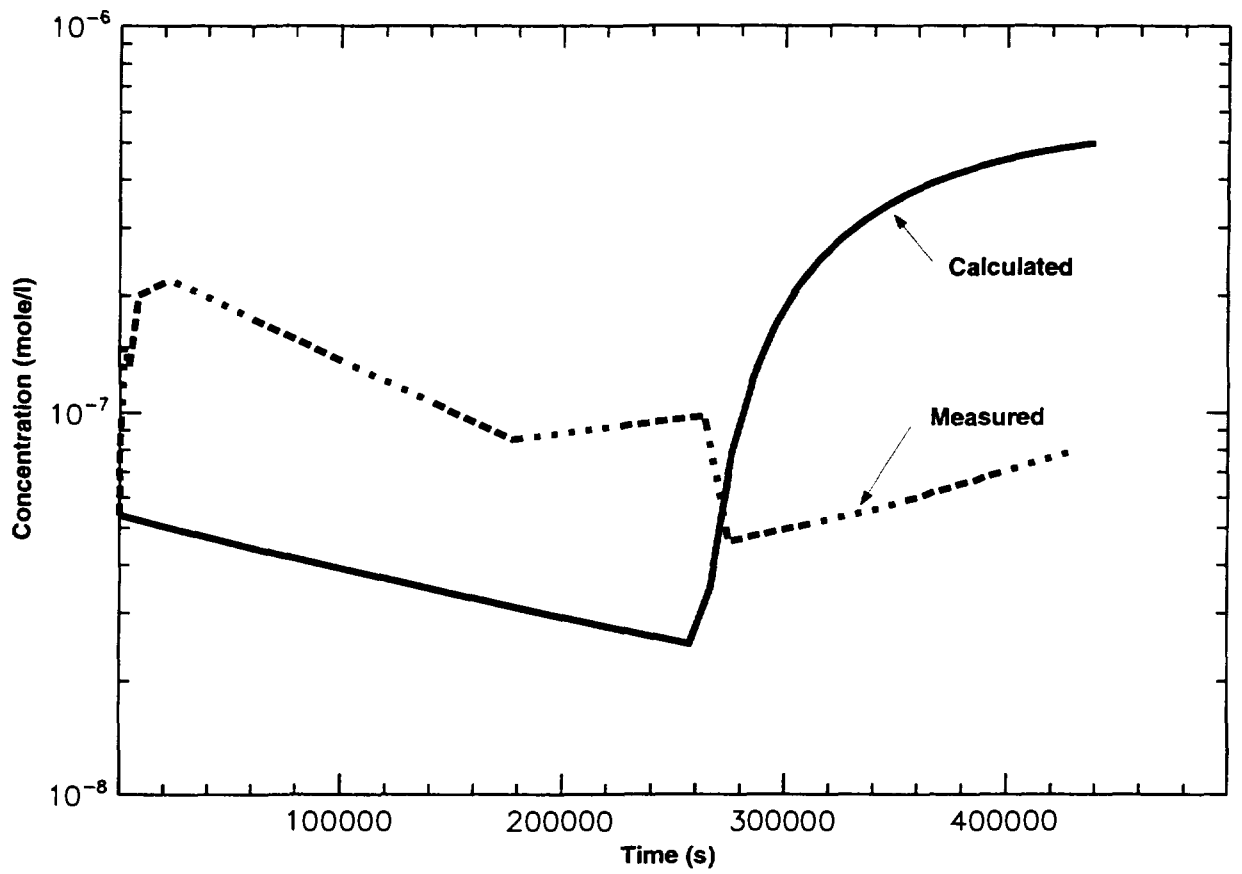


Figure 7: ACE/RTF3: Iodate Concentrations in the Water Space

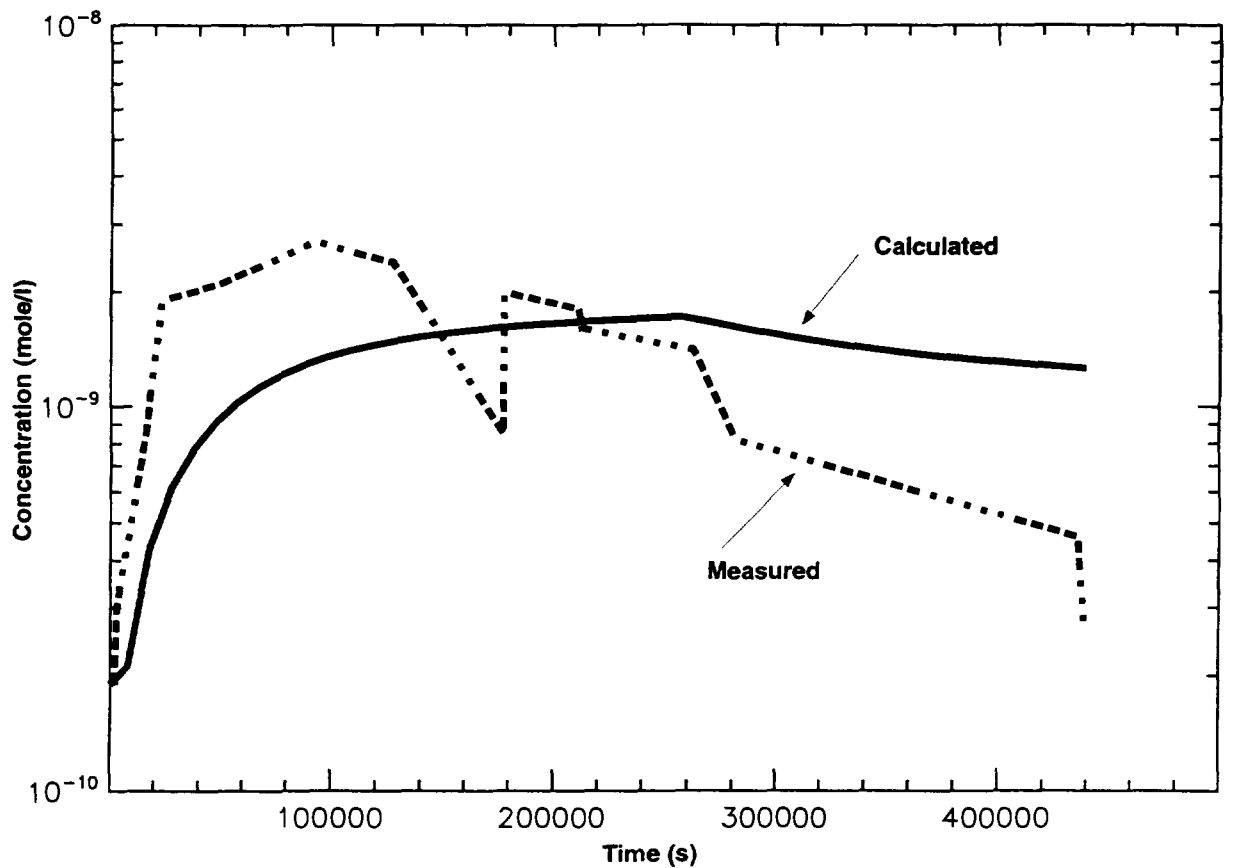


Figure 8: ACE/RTF3: Total Organoiodid Concentrations in the Gas Space

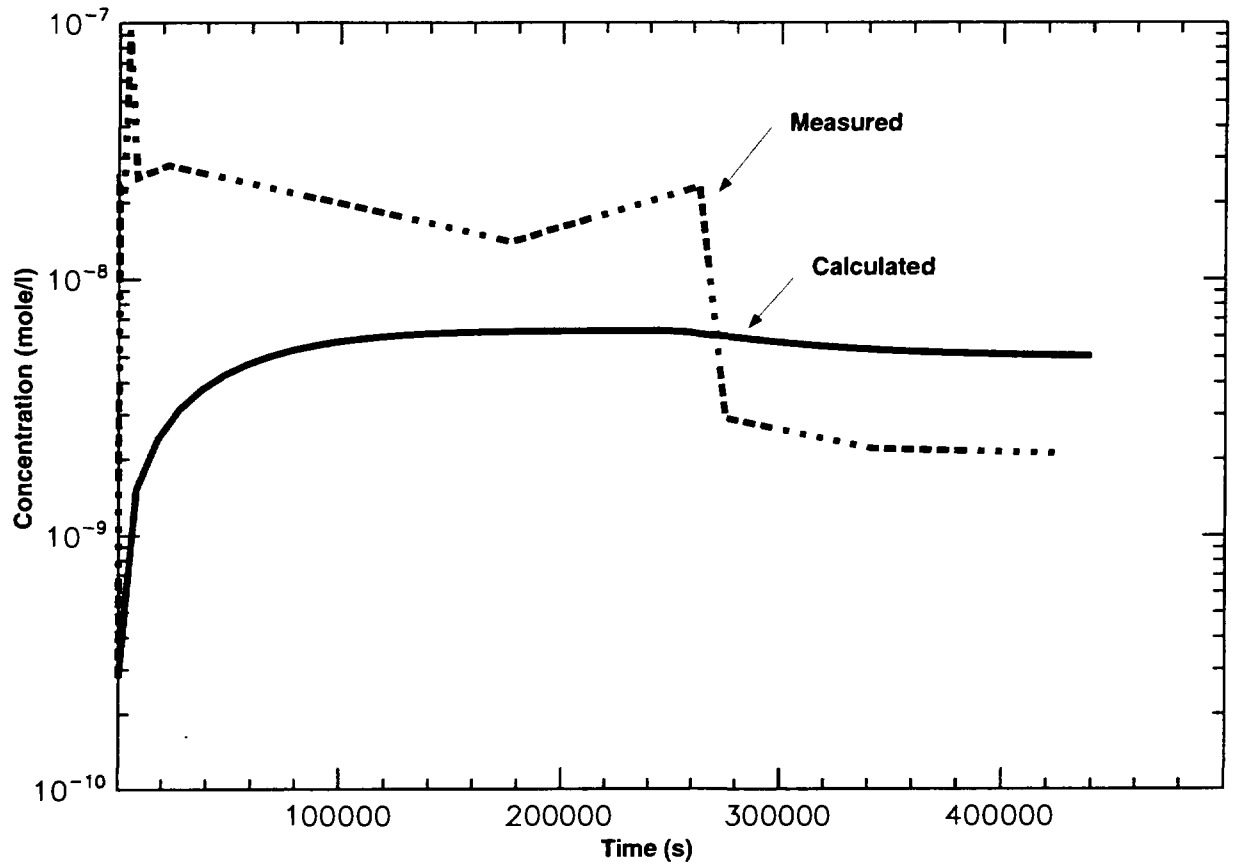


Figure 9: ACE/RTF3: Total Organoiodid Concentrations in the Water Space

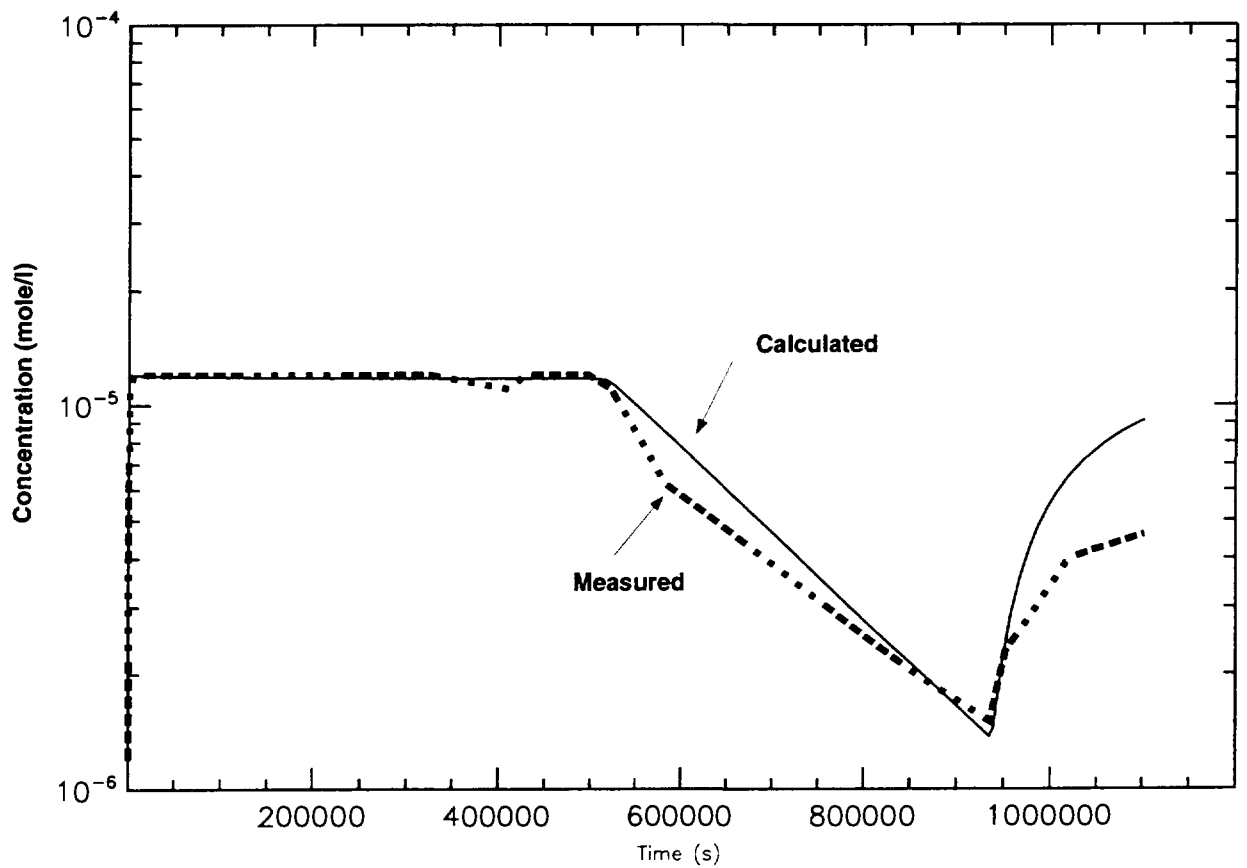


Figure 10: ACE/RTF 4: Iodide Concentrations in the Water Space

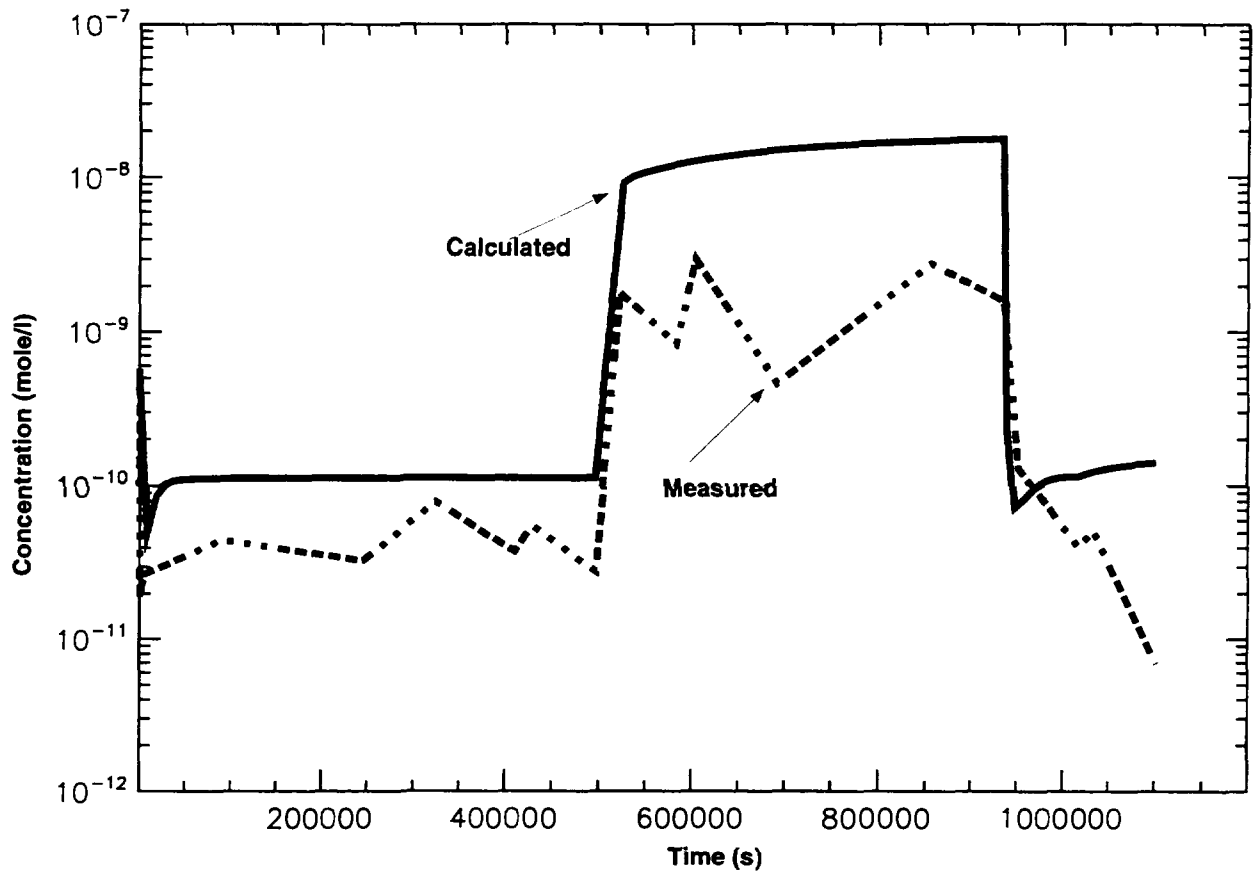


Figure 11: ACE/RTF 4: Molecular Iodine Concentrations in the Water Space

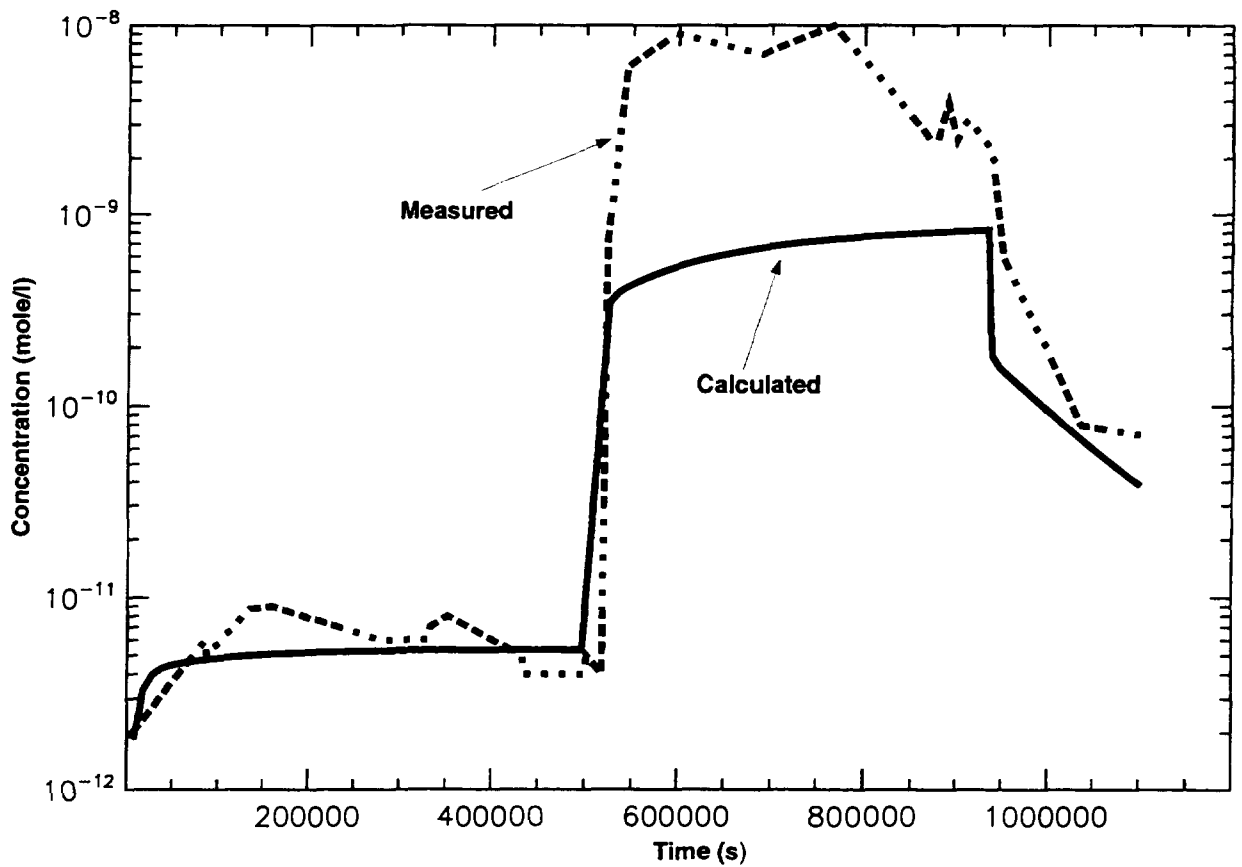


Figure 12: ACE/RTF 4: Molecular Iodine Concentrations in the Gas Space



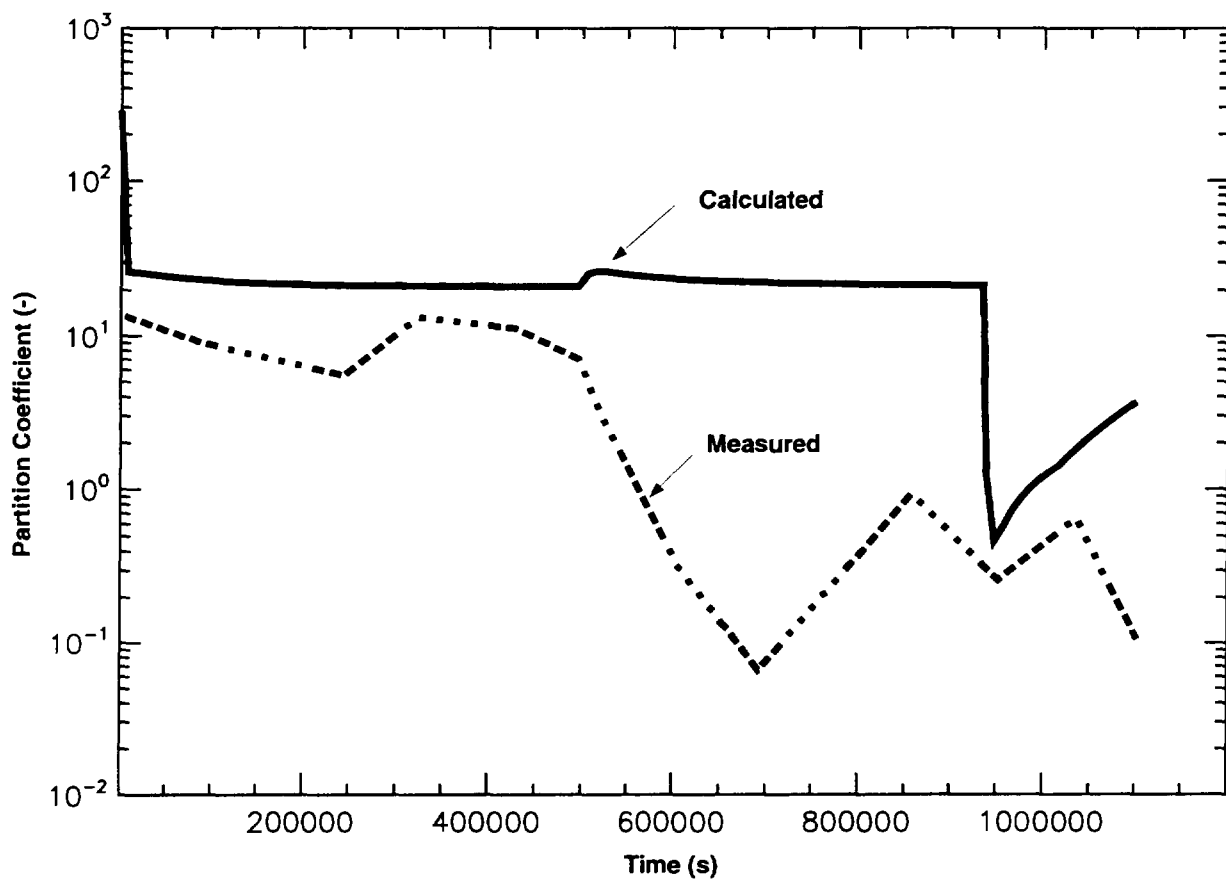


Figure 13: ACE/RTF 4: Molecular Iodine Partition Coefficients

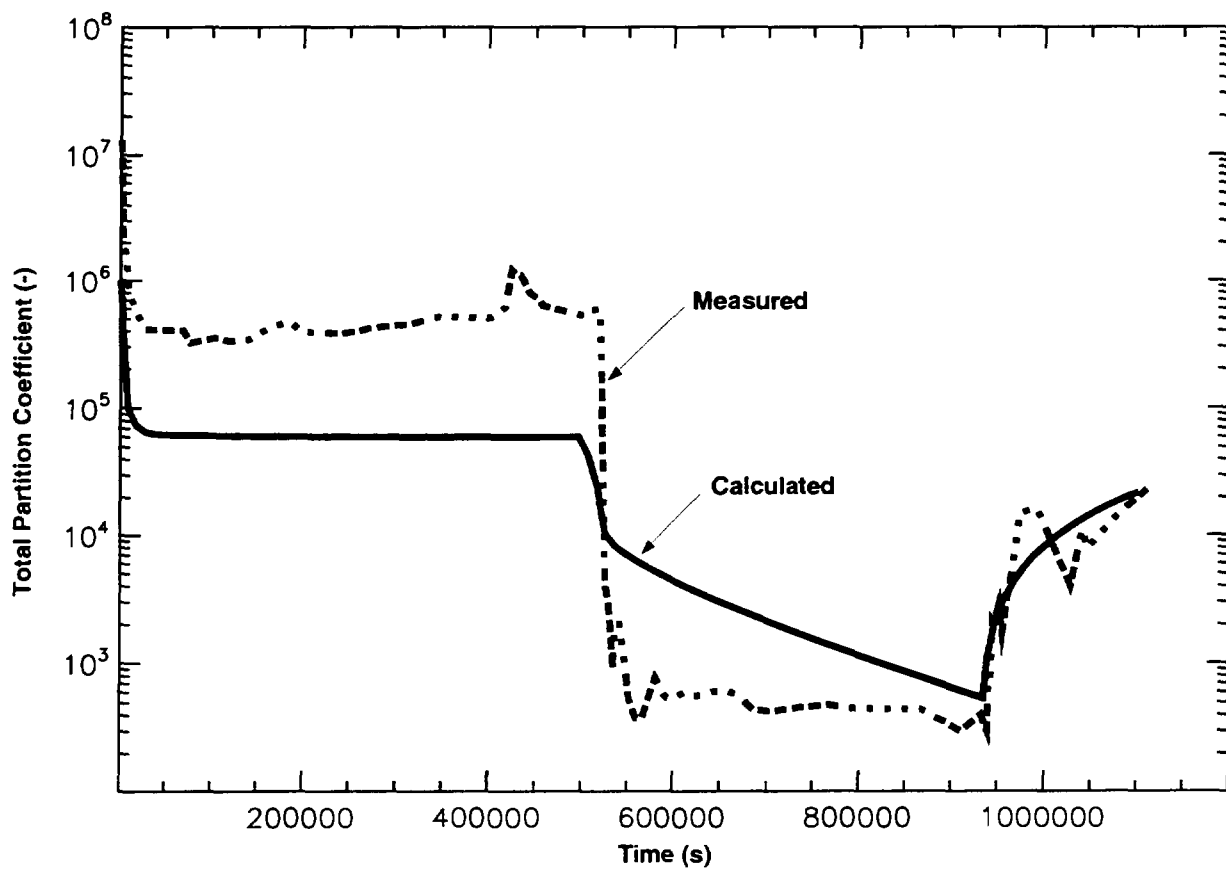


Figure 14: ACE/RTF 4: Total Iodine Partition Coefficients

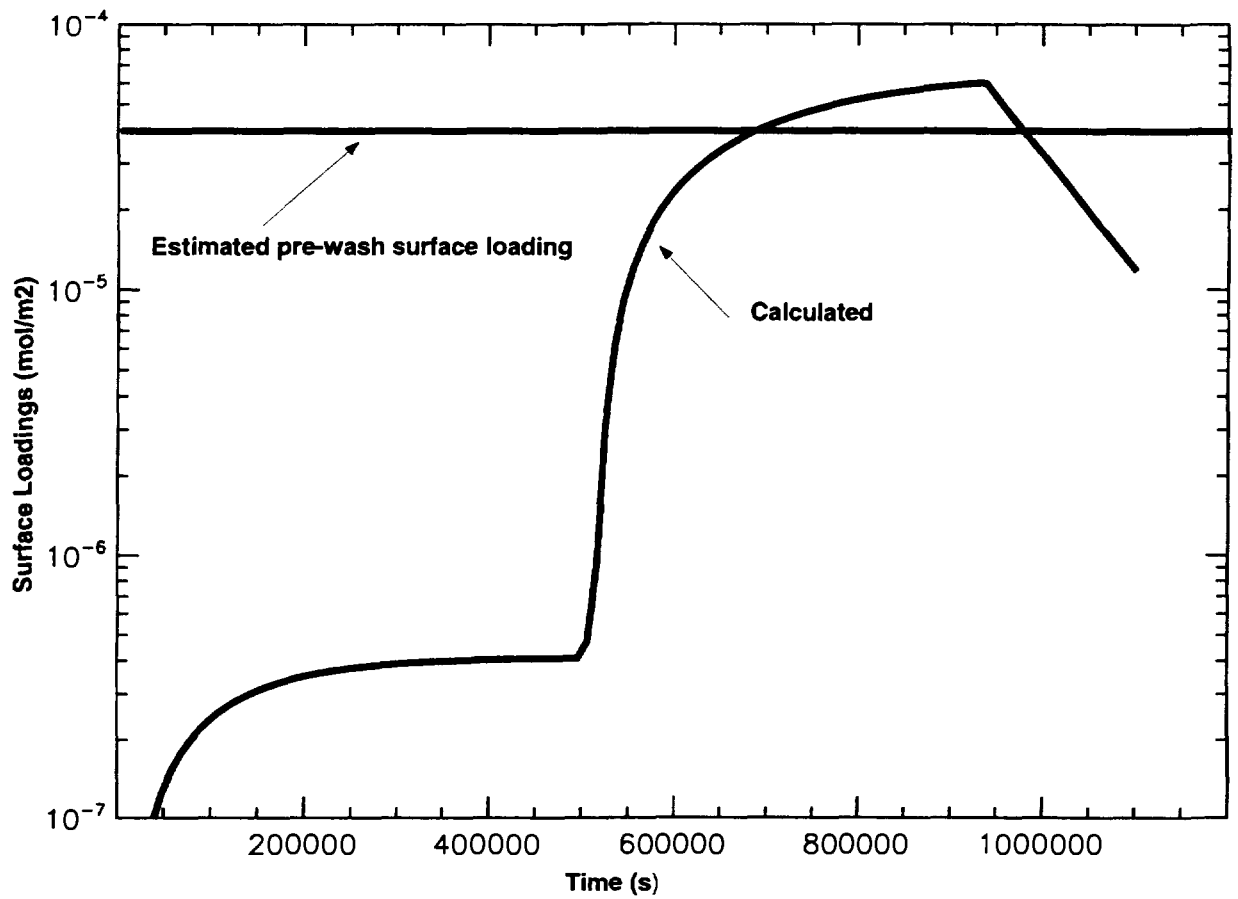


Figure 15: ACE/RTF 4: Surface Loadings on the Steel Surface in the Gas Space

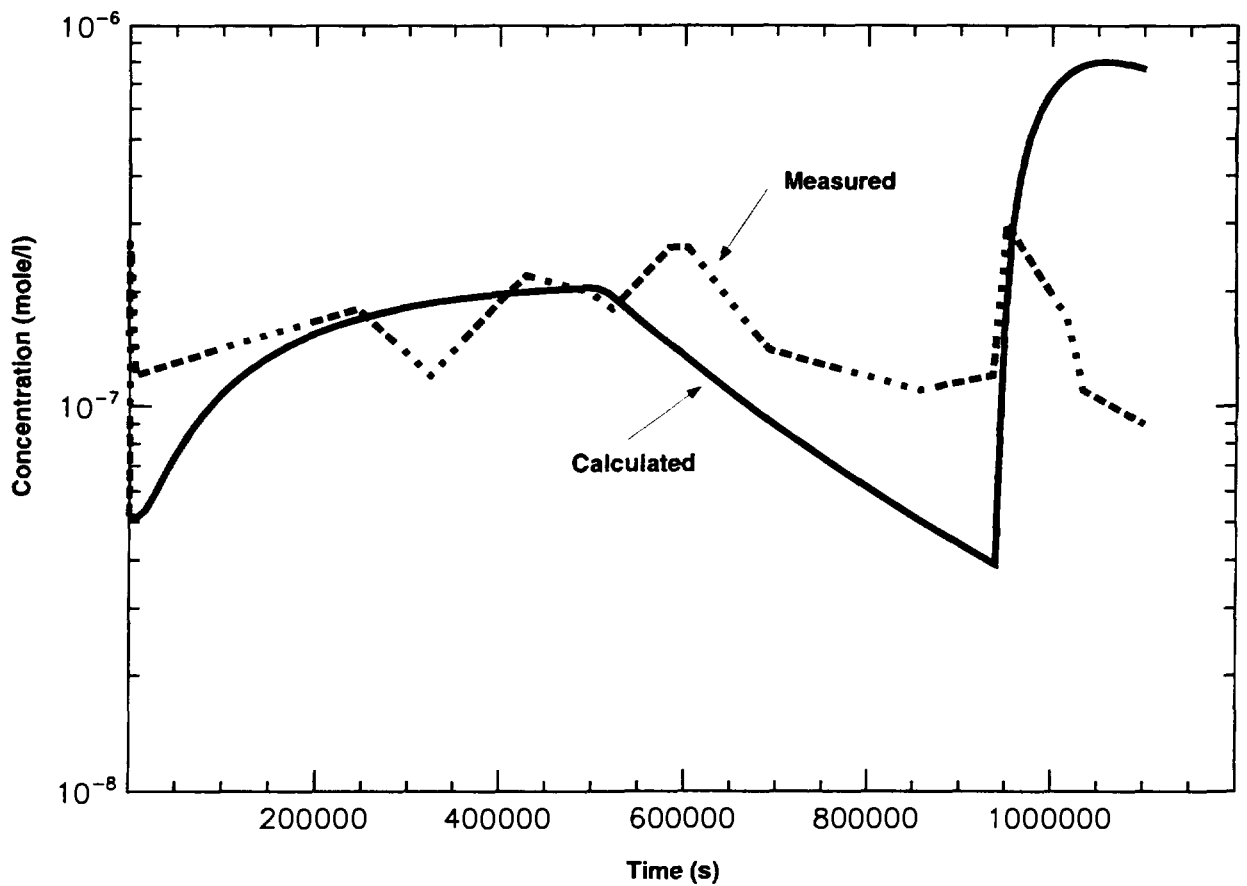


Figure 16: ACE/RTF 4: Iodate Concentrations in the Water Space

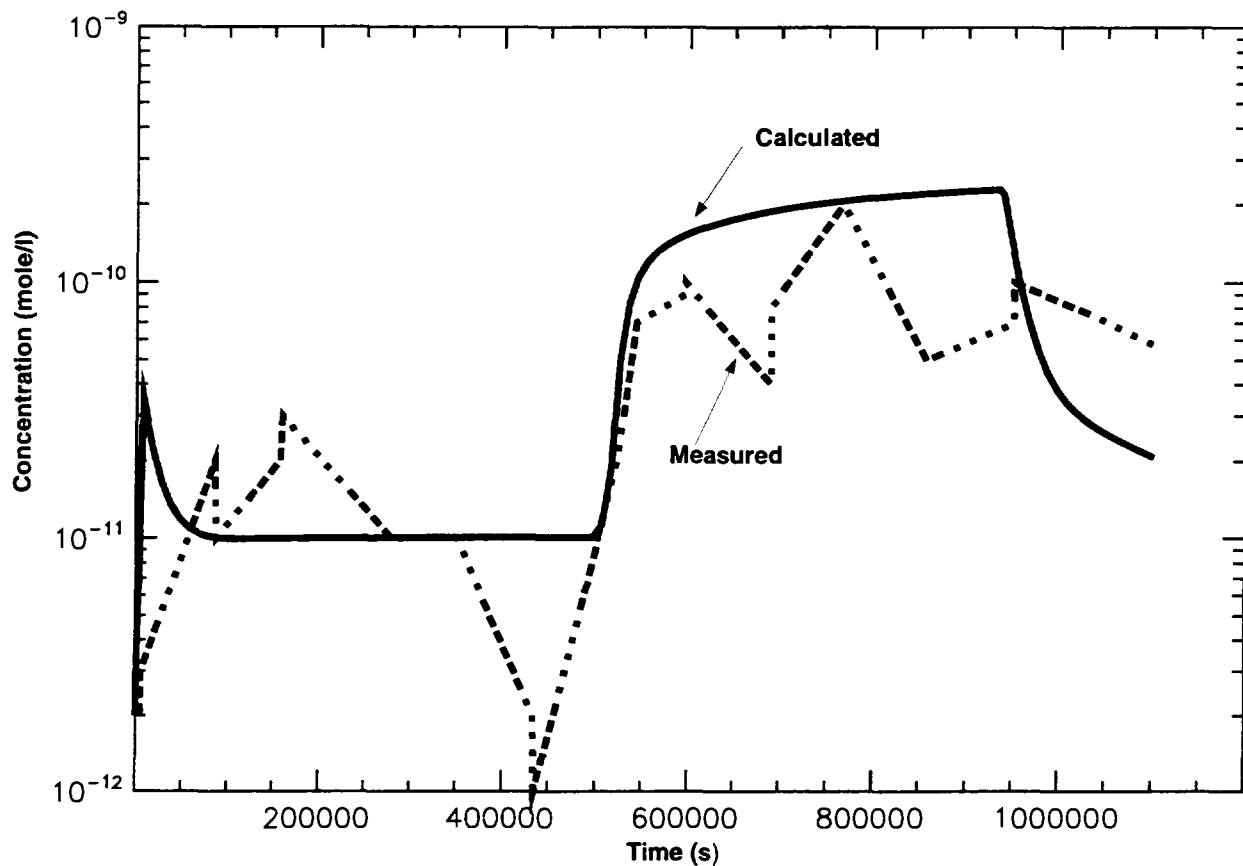


Figure 17: ACE/RTF 4: Total Organoiodide Concentrations in the Gas Space

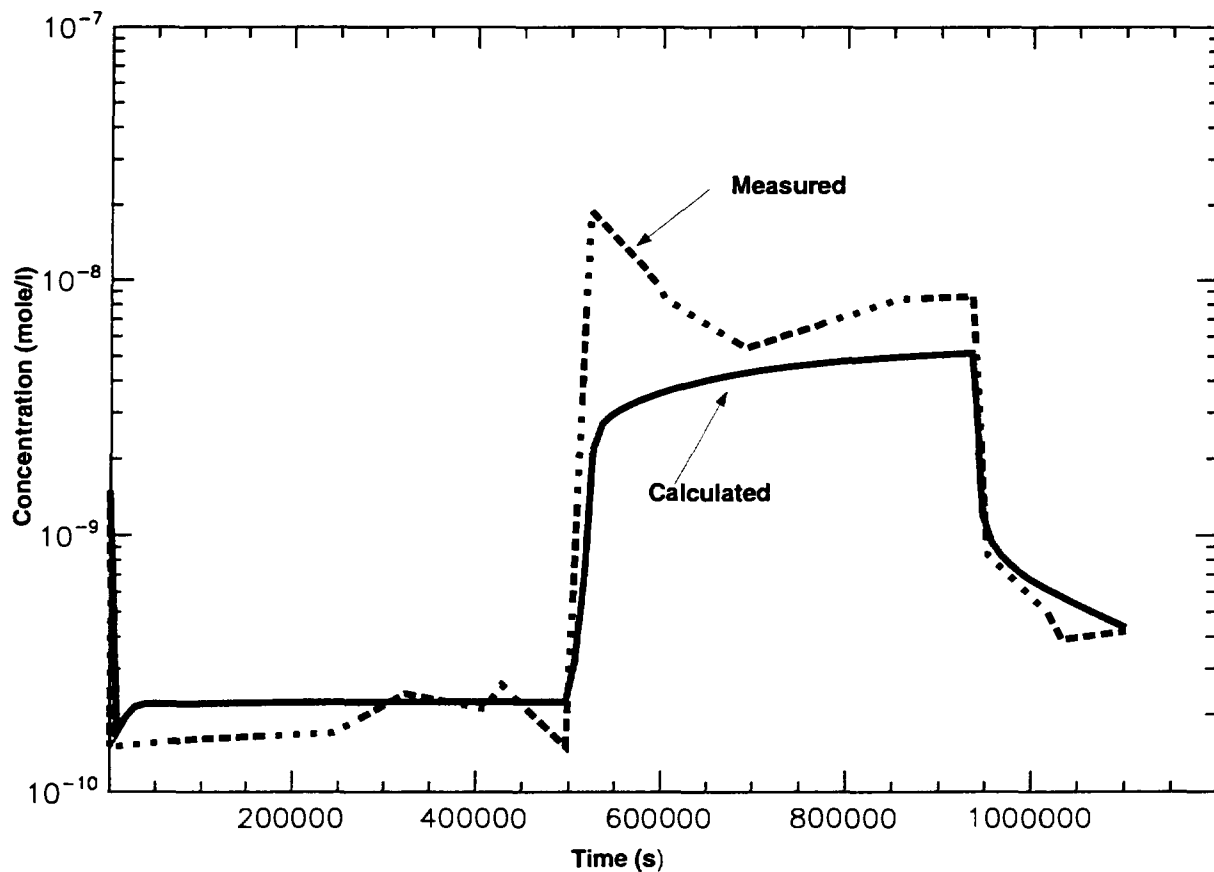


Figure 18: ACE/RTF 4: Total Organoiodide Concentrations in the Water Space